EXPERIMENTS WITH INCREASED VERTICAL RESOLUTION IN THE ECMWF ANALYSIS SYSTEM

J.H.Andersen

European Centre for Medium Range Weather Forecasts
Reading, U.K.

1. INTRODUCTION

The ECMWF forecasting model has a detailed vertical discretisation in the planetary boundary layer (PBL). It it a requirement for the calculation of surface fluxes following the Monin-Obukov similarity theory, that the lowest σ-level is located not more than 30 m above the ground, consequently 3 of the model's 15 layers are located in the PBL region. For the details of the physical parametrisation, see Tiedtke et. al. 1979.

The ECMWF analysis system operates on the 15 WMO mandatory standard levels, selected for economy in the exchange of meteorological information. However a considerable amount of significant level data from radiosondes is now available over the GTS network; at ECMWF this information is widely used for quality control. This paper reports on an experiment in the more direct use of off-level data by means of an increase in vertical resolution. The principles for the ECMWF data assimilation (DA) system are detailed in Lorenc et. al. 1977 and Lorenc 1981. A documentation of the status of the current DA-system is available from ECMWF.

2. VERTICAL INTERPOLATION PROBLEMS AND SPIN-UP TIME

From some of the Centre's early forecasting experiments, the so called spin-up problem was a noticeable feature of the medium range forecasts, Bengtsson, 1980. The naming of the effect came from the experience that it took about 3-5 days for the model to reach global equilibrium values for the heating by surface fluxes and cooling from radiation and large scale release of latent heat. Bengtsson found a large reduction in the spin-up time as a result of using the method of interpolation of analysis increments between the pressure surfaces of the analysis and the σ-surfaces of the model, instead of the previous full-field vertical interpolation, i.e. interpolation of the analysed fields rather than the departures from the first guess.

In December 1980, this method was introduced into the operational DA-system, the main reasoning being that the former full-field interpolation destroyed any boundary layer structure which was build up by the model. In data sparse areas it is an advantage to preserve the PBL; the impact of observations on the PBL in data dense areas is at most indirect. The model is said to have 'its own' PBL structure. However, one might fear that erroneous structures could persist by the use of the increment interpolation method.

2.1 Vertical resolution for the interpolation

In order to get an idea of the limitations imposed by the vertical interpolation, an idealised analysis step was performed as follows. Suppose we have a temperature field on the model's σ-layers as a first guess which happens to match the atmosphere exactly ;the dotted curves Figs. 1-4. The field is then transformed to heights on pressure levels. For the 15 level analysis system, the levels are: 10, 20, 30, 50, 70, 100, 150, 200, 250, 300, 400, 500, 700, 850 and 1000 mb. With the increased vertical resolution, four extra levels are introduced : 600, 800, 900 and 950 mb; this system is referred to as the 19 level (19L) analysis system.

We can assume without loss of generality that the first guess heights matches the atmosphere exactly by virtue of an unknown inter-level temperature distribution. This fortunate situation, however, is rather unlikely; an erroneous first guess is therefore simulated by superimposing a vertical 2-grid wave on the temperature profile, as shown by the thick curve of Fig. 1. This error mode is characteristic for most vertical discretisation schemes, although the amplitude (2 K) is exaggerated, note also the positioning of the σ-levels highlighted by the wave.

By following through the analysis process, we generate height increments on pressure surfaces, which are transformed into temperature increments on σ-surfaces. The resulting 'analysed' profile is shown in Fig. 3. The error is markedly damped above 350 mb where the concentration of analysis levels is high. However for σ-levels 4, 6 and 9 numbered from the bottom, the first guess error is amplified. Fig. 4 shows the interpolation cycle performed by a 19 analysis level system; it is clear that the boundary layer structure is much better reproduced, though the error now amplifies for σ-levels 1 and 9.

A schematic representation of the vertical interpolation test is shown below. T' is the perturbed first guess temperature which is transformed to Z'; the heights on pressure levels and used as a background field (first guess) for the assumed true height field Z. The resulting increment ΔZ is transformed back to σ-levels and used to rectify the T' field (analysing the true temperature field).

1. $T(\sigma)$ true $\rightarrow$ $Z(p)$ true
2. $T'(\sigma) \rightarrow Z'(p) \longrightarrow \Delta Z(p) \rightarrow \Delta T(\sigma)$
3. Compare $T(\sigma)$ with $T'(\sigma) + \Delta T(\sigma)$

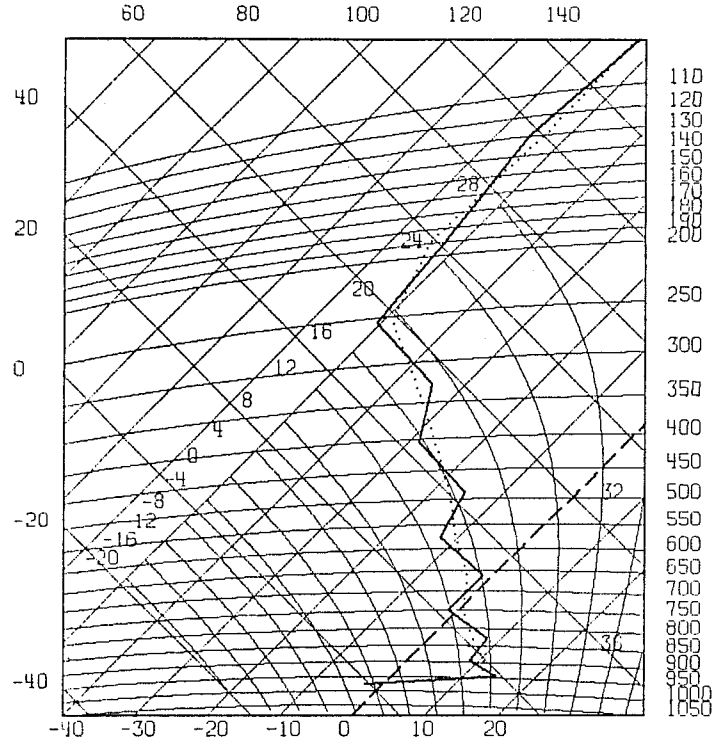

Fig. 1 Tephigram for (true) first guess temperatures (dotted line) and for super-imposed error mode (full line).

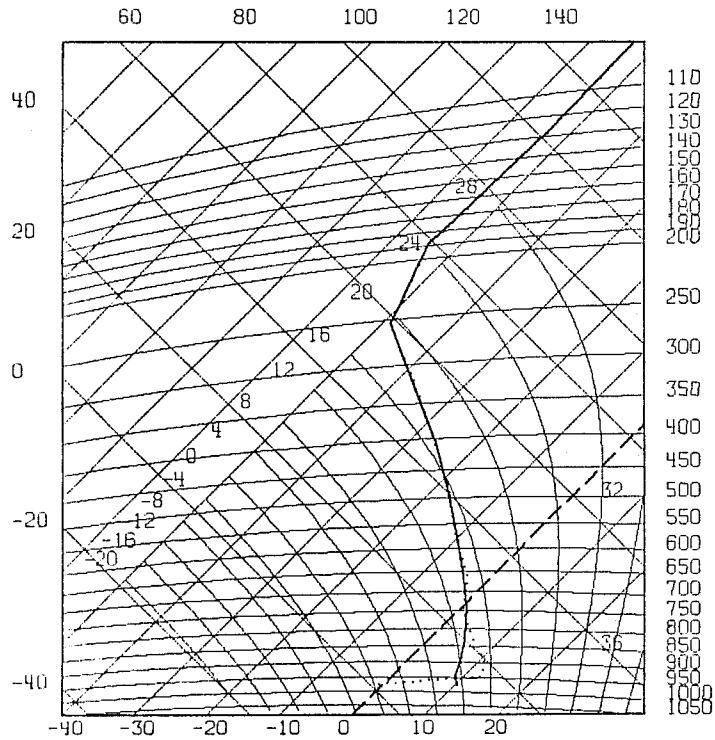

Fig. 2 Tephigram for (true) first guess temperatures (dotted line) and after a full field interpolation cycle (full line).

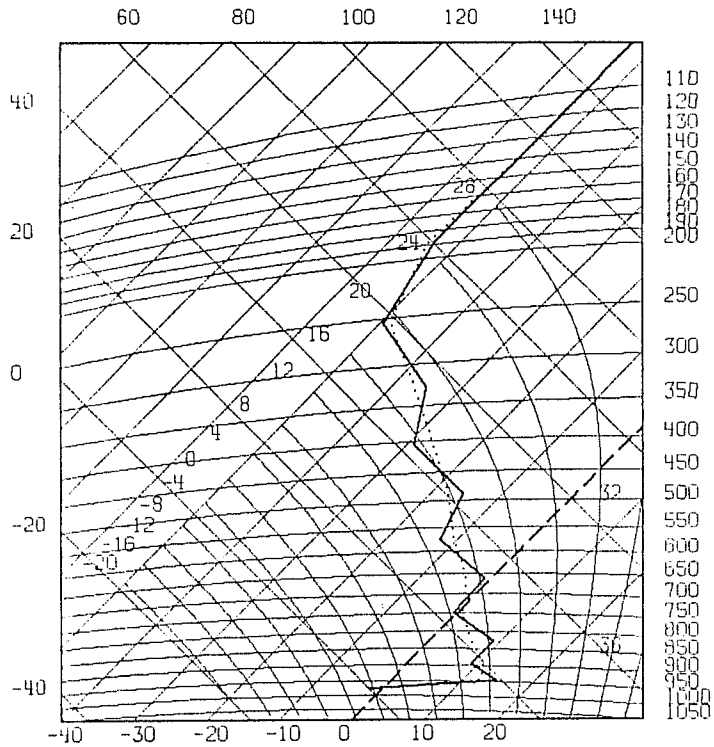

Fig. 3 Tephigram for (true) first guess temperatures (dotted line) and the rectified profile using a 15-level increment interpolation cycle (full line).

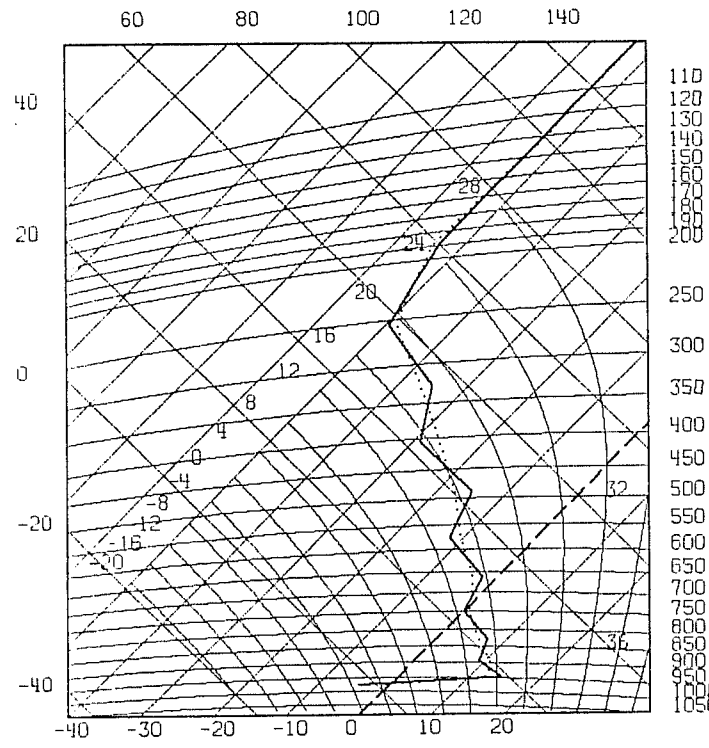

Fig. 4 Tephigram for (true) first guess temperatures (dotted line) and the rectified profile using a 19-level increment interpolation cycle (full line).

The unperturbed first guess temperature profile was taken from a gridpoint in Asia (60° N, 60° E), where the profile was inadequate because the model fails to dispose of a strong surface inversion, mainly due to the lack (presently) of a diurnal cycle. In Fig. 2 the result of a full-field interpolation cycle can be seen to effectively 'initialise' the boundary layer. This method was used for the FGGE III-B analyses at ECMWF, Bjornheim et.al. 1981. It was justified because the analyses are likely to be used as initial data for models with a range of alternative physical parametrisation schemes.

3. DATA AVAILABILITY

The main data source for the extra-level analysis is at present the radiosondes: TEMP's and PILOT's. When integrating the hydrostatic equation, care must be taken to ensure compatability with the set of standard level heights. In the experimental analysis, the nearest standard level height was used as reference if it was within 100 mb of the extra level under consideration. Then the virtual temperatures were scanned; if the nearest significant level temperature level was more than 50 mb from the extra level, the attempted integration was abandoned. These conditions were set in order to avoid filling up the optimum interpolation (O/I) matrices with obviously redundant information.

The vector winds at analysis levels were obtained from the radiosondes by means of a filtering operation - the exact details are given in part 4. The main idea is that the linear momentum of the vertical column is conserved under the truncation process of mapping a high resolution wind profile onto the analysis levels.

Table 1. shows a typical count of radiosonde data (12Z on the 28 April 1982). It includes only the data actually used by the analysis; furthermore the superobservations are counted as single observations.

MB	TEMP Z		TEMP (u,v)		PILOT (u,v)	
	19L	15L	19L	15L	19L	15L
1000	443	568	240	524	0	1
950	327	-	16	-	1	-
900	253	-	26	-	2	-
850	572	601	547	587	181	182
800	273	-	125	-	2	-
700	586	605	582	597	128	128
600	285	-	132	-	2	-
500	601	621	592	604	81	82

Table 1
Counts of radiosonde data used by 19L/15L analysis on 12Z 28/4-1982

The small number of extra level radiosonde winds at 950 mb and 900 mb is due to a somewhat restrictive use of the filtering operation; if an analysis level had no wind report, significant wind levels were required on both sides of the analysis level and within 60% of the pressure intervals. When using FGGE observational data from the global experiment in 1979, it was found that the extra levels winds could be constituted from radiosondes, typically with 2/3 of the number of standard level data. The much larger number of extra heights are counterbalanced by the vertical observation error correlation function for the heights. As close vertical neighbours are highly correlated, the O/I tends to suppress the neighbours as redundant information. Presently, we assume that the wind observation errors are vertically uncorrelated.

The data counts from SYNOP's and SHIP's are shown in Table 2. Here the wind observations are simply assigned to the level nearest to the first guess surface pressure, hence the comparatively large number of 950mb winds. The drop in data counts for the 19L heights is due to the avoidance of PMSL data reduced over more than 800m from the station level, and surface pressure data where the station level departs by more than 800m from the model topography.

MB	SYNOP/SHIP Z		S/SH (u,v)	
	19L	15L	19L	15L
1000	2548	3186	2240	3025
950	6	-	627	-
900	3	-	98	-
850	181	225	34	233
800	15	-	9	-
700	36	62	5	10
600	16	-	1	-

Table.2

Counts of SYNOP/SHIP data used by 19L/15L analysis on 12Z 28/4-1982

MB	SATOB (u,v)	
	19L	15L
900	344	-
850	99	443
300	55	55
250	7	7

Table.3

Counts of cloudwind data used by 19L/15L analysis on 12Z 28/4-1982

Table 3 shows that the 19L analysis is benefitting from the reassignment of most SATOB cloudwinds from 850 mb to 900 mb, the preferred reporting level for the GOES geostationary satellites. The DA-system normally transports a single level wind report to the nearest analysis level via the first guess gradient, hence the uncertainty which comes from this blending of the first guess with an observation is greatly reduced.

The NOAA-6 and 7 satellites do not resolve the thicknesses between the extra levels in the high resolution analysis. The operational analysis system can only handle thicknesses between adjacent analysis levels, any thickness covering more than one analysis level is broken up into independent observations. Operationally, the first guess is used to scale the sub-thickness if required. However, this method affects the stability of the sub-layers. For the 19 level system the method of breaking up the SATEM thicknesses was changed, so that the same temperature increment was assumed for each sub-layer. Furthermore, the observation error was inflated in order to counteract the advantage of the artificial increase in observational data.

4. THE MOMENTUM FILTER

A method has been developed for the pre-analysis mapping of a detailed wind profile onto the analysis levels. In contrast to an ordinary interpolation, the method integrates all the observed information, thereby conserving the integral of linear momentum of the profile. The method is also consistent, i.e. the filtering has no effect if the profile consists of analysis levels only. In general terms, the filtered wind vector at analysis level j can be expressed as:

$$\underline{V}_j = \frac{1}{N_j} \int_0^{1050} \underline{V}_s(p)\, F_j(p)\, dp \qquad (1)$$

where $\underline{V}_s$ is the observed profile of line segments, F_j is the j'th filter function and N_j is the normalisation integral.

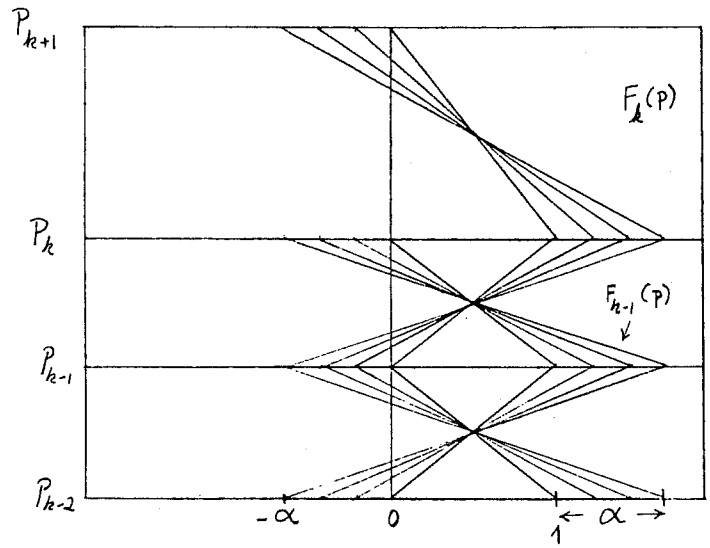

Fig. 5 Localised filter functions for pre-analysis of radiosonde wind-profiles, the filtering is neutral for $\alpha = 1$.

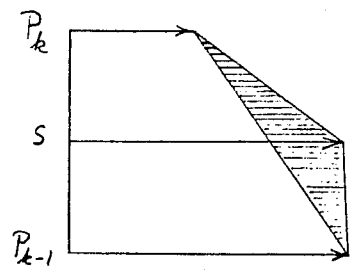

Fig. 6 If the significant level wind observation at S is ignored, the momentum represented by the shaded area is lost.

By requiring the momentum sum of the l.h.s of eq.(1) be equal to the original momentum integral, an integral equation arises. The kernels of the two sides must be equal, hence the following condition holds:

$$\frac{1}{2} \sum_{j=1}^{NA-1} \left(\frac{F_j(p)}{N_j} + \frac{F_{j+1}(p)}{N_{j+1}} \right) \quad (p_j - p_{j+1}) = 1 \qquad (2)$$

where NA is the number of analysis levels. Furthermore, the filters should be localised; they should not extend beyond the neigbouring levels. For a selected interval $[p_k, p_{k+1}]$, this means that at most 3 terms from the sum (2) contribute. By some rather lengthy calculations, the following two statements can be proven:

$$N_k = \frac{1}{2} (p_{k-1} - p_{k+1}) \quad \text{and} \quad F_k(p) + F_{k+1}(p) = 1 \qquad (3)$$

It is convenient to construct the filters by means of line segments; some possible filters which obey (3) are shown in Fig. 5. The parameter α should be chosen such that the filter operation becomes neutral for a profile at analysis levels, this is the case for $\alpha = 1$. However, it then follows that the filtering is also neutral for any report where the observed winds fall onto the line segments connecting the analysis levels.

Apart from the function of mapping onto the extra levels, it is envisaged that the filtering method could give a more faithfull representation of the strength of the winds near the jet-stream levels. This simple idea is demonstated by Fig. 6, the shaded area of the figure shows the observed amount of linear momentum, which would be lost in the aliasing process; the filtering method distributes this excess momentum to the appropriate levels. Fig. 7 shows an example of the filtering applied to a typical TEMP over Japan

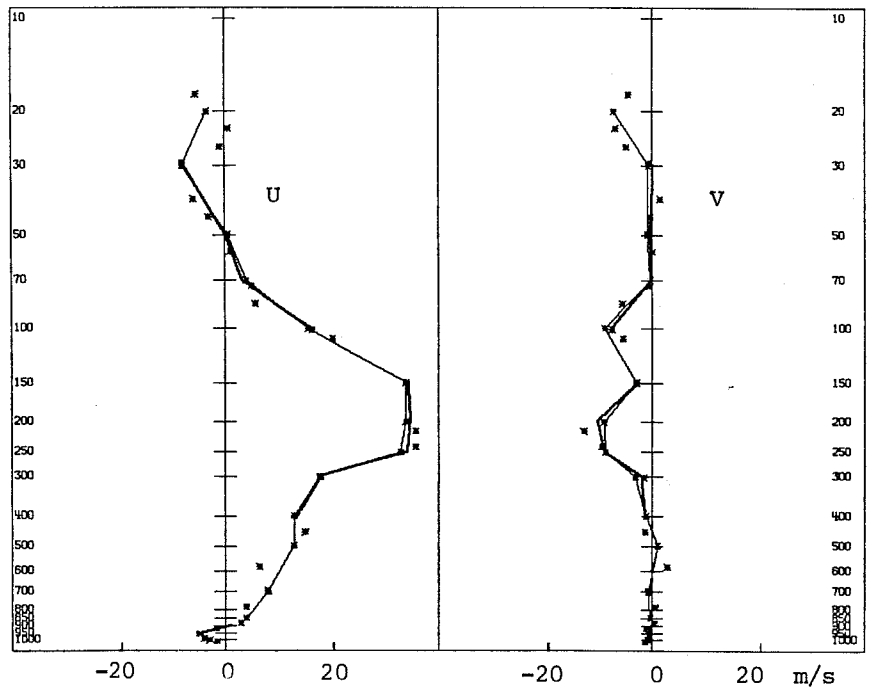

Fig. 7
A demonstration of the momentum filter for a radiosonde over Japan. Thin lines are connecting the standard level data, thick lines are momentum filtered where possible.

The thick curves are momentum filtered sections where the off-level data contributes. The soundings from the Omega wind finding system are often more detailed; as many as 80 wind levels has been received, but most of these data are lost by the conventional data selection.

5. VERTICAL RESOLUTION OF THE OPTIMUM INTERPOLATION (O/I) ANALYSIS

The question naturally arises as to whether the O/I system can respond to a higher resolution when the presently assumed statistical tables for the observation and prediction error covariances are used.

The vertical prediction error correlations (P) are based on those of Hollett, 1975. He computed values for a 5-level primitive equation model by splitting the covariances into horizontal and vertical components. The resulting vertical correlation matrices were extrapolated at ECMWF from 100 mb and up to 10 mb; the main features of Hollett's values were retained, including an apparent rise in correlation between the bottom and the top level (100 mb). Lonnberg, 1982, have recently found an alternative method for the splitting of the error covariances into contributions from predictions and observations. His latest results are due for implementation into the ECMWF operational DA-system.

All examples of one column O/I discussed in the following refers to a 19L analysis for 12Z on the 29 April 1982 at 45°N, 0°W. Fig. 8 shows the correlation matrix $\underline{\underline{P}}$ relating to the April climatology. The same correlations are assumed for heights and winds; the behaviour in the stratosphere is fairly typical for other months and geographical locations. Operationally, the 15 by 15 level submatrices are used.

A requirement for solving an O/I problem is the specification of the matrix $\underline{\underline{M}}$ which contains the statistical information, see Lorenc et.al. 1977.

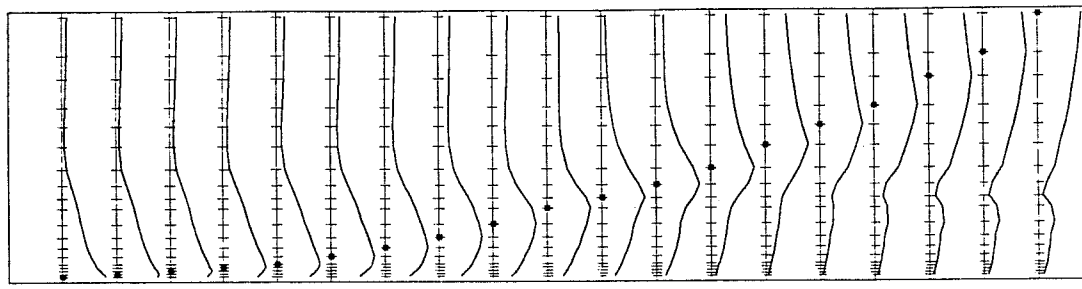

Fig. 8 Z/Z and $\bar{v}/\bar{v}$ prediction error correlations (see text)

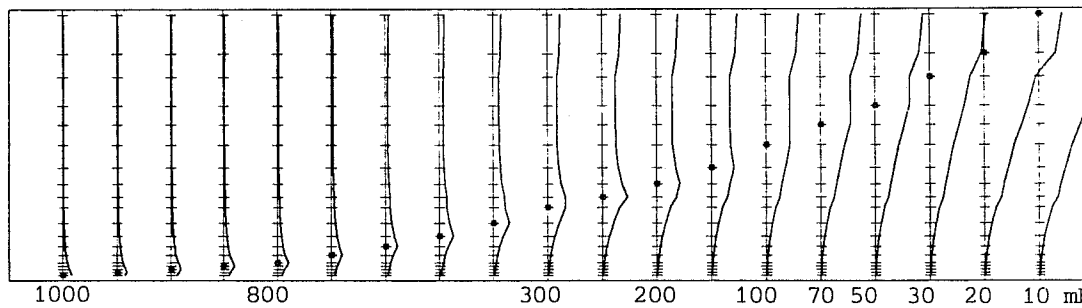

Fig.9 Scaled observation error correlations for heights(TEMP)

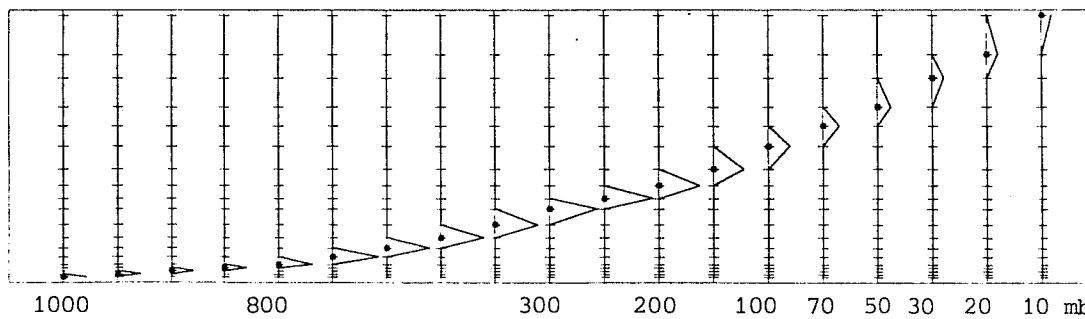

Fig. 10 Scaled observation error correlations for winds (TEMP)

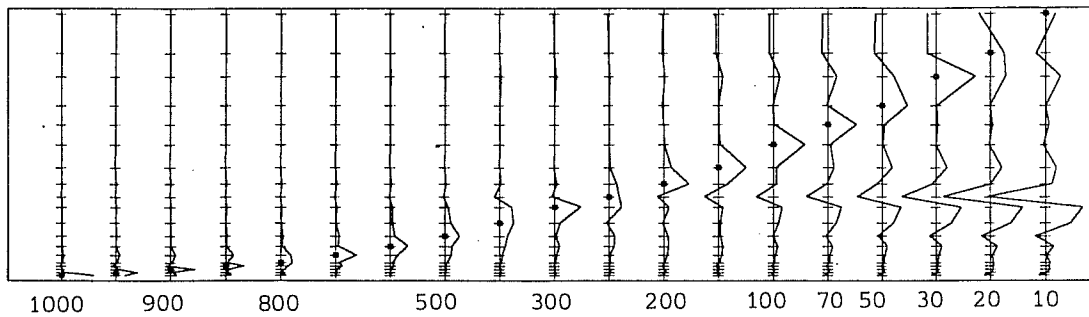

Fig. 11 Vertical contributions to the height analysis at the dotted point from height observations (TEMP)

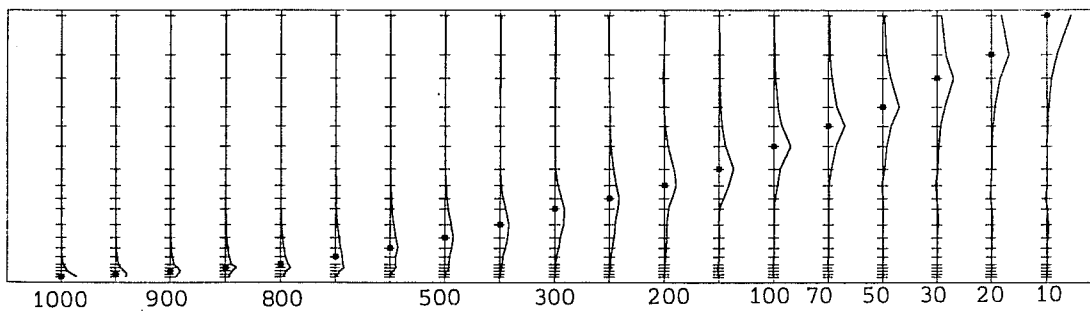

Fig. 12 Vertical contributions to the wind analysis from wind observations (TEMP)

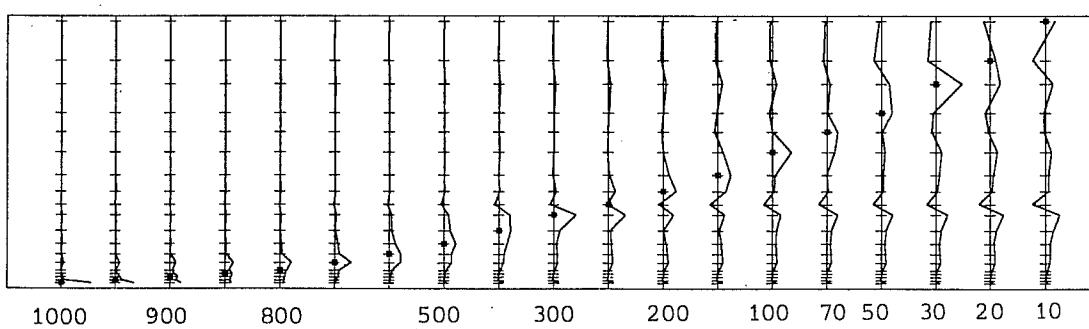

Fig.13 Vertical contributions to the height analysis from height observations with thickness data available.

$$\underline{\underline{M}} = \underline{\underline{P}} + \underline{\underline{O}} \qquad (4)$$

$\underline{\underline{P}}$ is the prediction error correlations and $\underline{\underline{O}}$ is the observation error covariances normalised by the first guess errors. The O/I solution for the analysis weights is:

$$\underline{\underline{W}} = \underline{\underline{M}}^{-1}\ \underline{\underline{P}} \qquad (5)$$

The result is a matrix $\underline{\underline{W}}$ of weights normalised by the first guess for the observed increments (column index) to generate the analysis increments (row index) The effect of the observation correlations is to suppress the neighbouring data as redundant information.

The examples of weight curves shown in Figs. 11 to 13 are all un-normalised, these weights could also be derived from (5) directly by using the covariances for the components of $\underline{\underline{M}}$. However, it is instructive to display the scaled observational matrix $\underline{\underline{O}}$; when this matrix is almost singular, then the stability of the numerical inversion of M becomes more sensitive to the tail end of the vertical prediction correlations.

Fig. 9 shows the height/height part of the matrix $\underline{\underline{O}}$, the slow decay seen in the stratospheric column is caused by the ascribed observation error; (in the stratosphere it exceeds the first guess error). The wind/wind part of the matrix $\underline{\underline{O}}$ is diagonal because of the assumption of uncorrelated observation errors.

The resulting vertical distribution of weights for the heights are shown in Fig. 11, the curves show the contributions to the analysis increment at the level indicated by a dot. Fig. 12 shows the weights for the winds. The weights are much more localised for the heights than for the winds, in fact in the boundary layers only height observations at the level analysed are significant.The observation correlation has the effect of suppressing the immediate neighbouring observations as redundant information; they cannot

contribute sufficiently in reducing the estimated analysis error variance. When thickness observations are included in the O/I problem, see Fig.13, weights are given to the neighbouring heights which become useful reference levels. The spurious peaks in the stratospheric height analysis from data around 300 mb is caused by the shape of the P-matrix (Fig. 8), however, the stratospheric analysis is only affected if data are selected at such levels.

6. EXPERIMENTAL RESULTS

A preliminary test of the 19-level analysis scheme was carried out; five analysis cycles were run from 12z on the 28 April 1982 to 12z on the 29 April. The forecasts from the end of the assimilation period were compared with the forecast from a 15 level control run, both forecasts were compared to the available ECMWF operational analysis. The control assimilation was distinct from the operational assimilation due to minor system changes. The changes to the default analysis system on 25th of May 1982 included new observation errors for the radiosonde winds and a revised buddy checking. Both experimental data-assimilations were started form climatology (coldstart) on the 28th of April.

The situation was chosen because of a rapid development of a frontal system centered over Iceland. In the 24 hour period from 12Z 29/4/82, the centre moved eastward to the Faroe Island. The cold outbreak gave snow in the north of Scotland. During the 24 hour period the mean sea level pressure (PMSL) of the depression dropped from 1002 mb to 987 mb. The minimum pressure forecast by the operational run was 995 mb. However, the forecasts from both the test and the control data-assimilation did not decrease the PMSL further. Although only few extra-level winds could be constituted from the available TEMP's and PILOT's, it was expected that the upper air winds would benefit from the integration of the significant level winds into the standard-level wind observations. Hence, amongst the multitude of areas which are affected by the experiment, we will only examine the forecasts of the 500 mb height

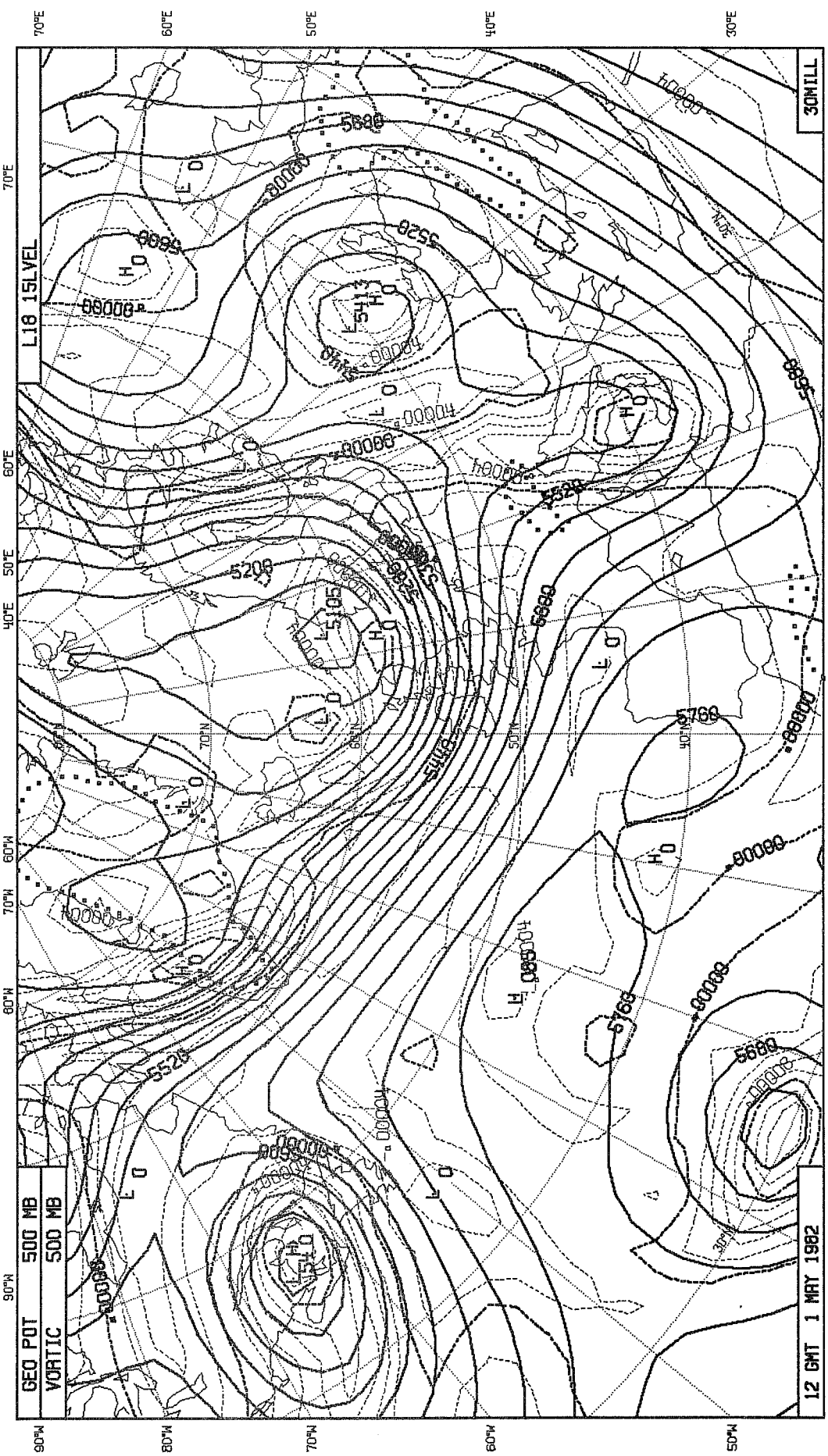

Fig. 14 48 hour forecast from initial data using a 15-level data assimilation.

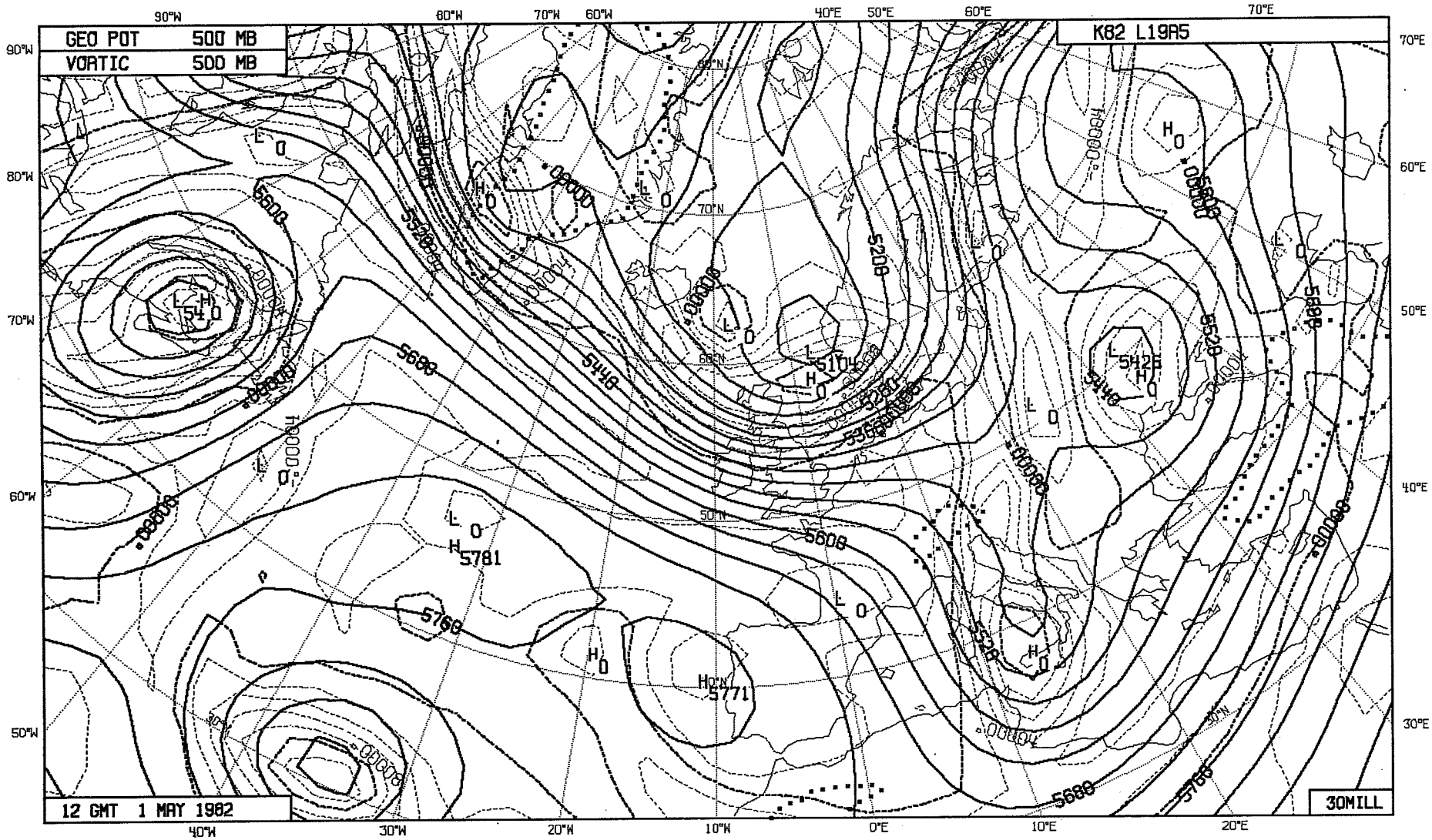

Fig. 15 48 hour forecast from initial data from a 19-level data assimilation.

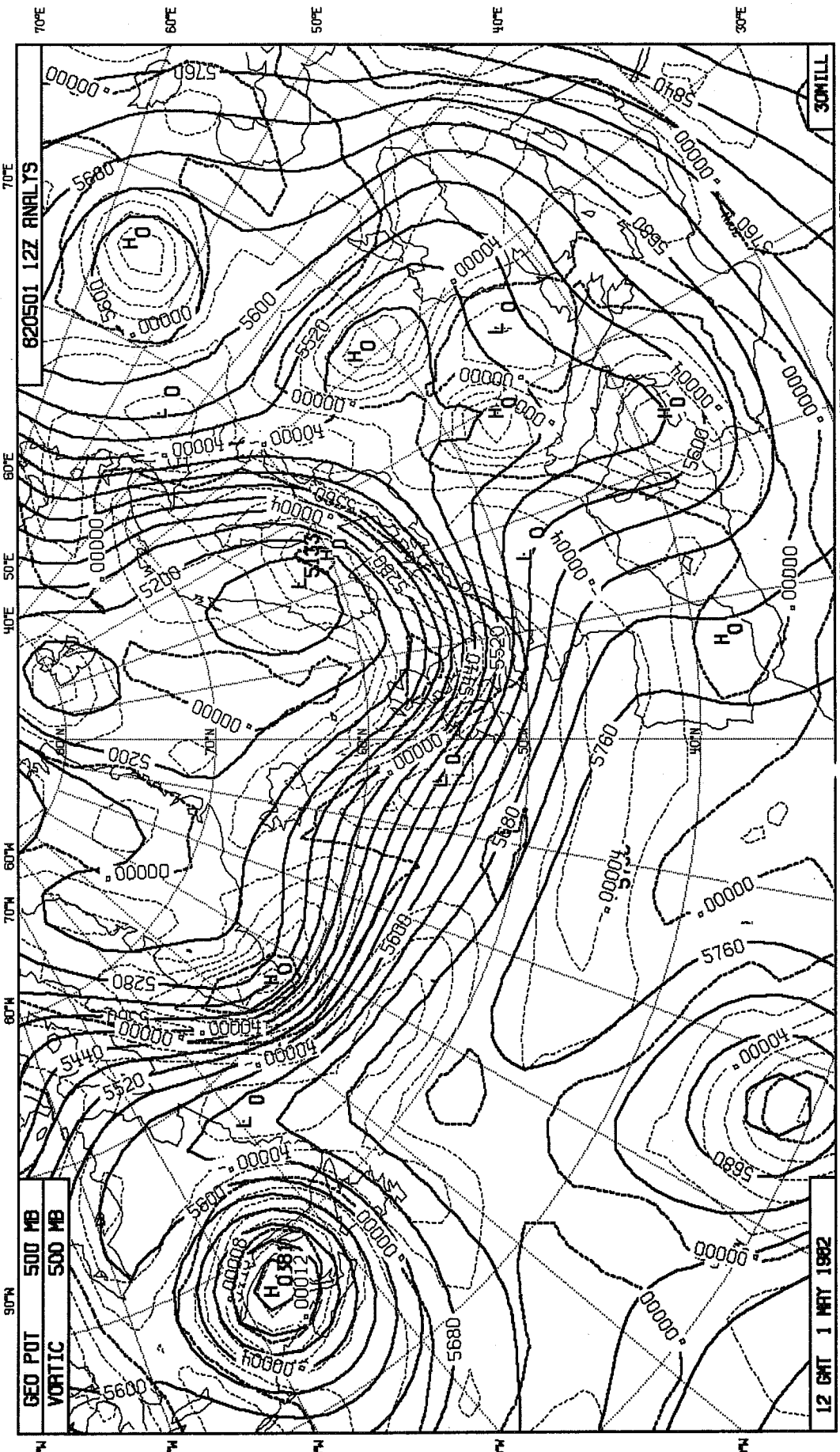

Fig. 16 ECMWF operational analysis at verifying time.

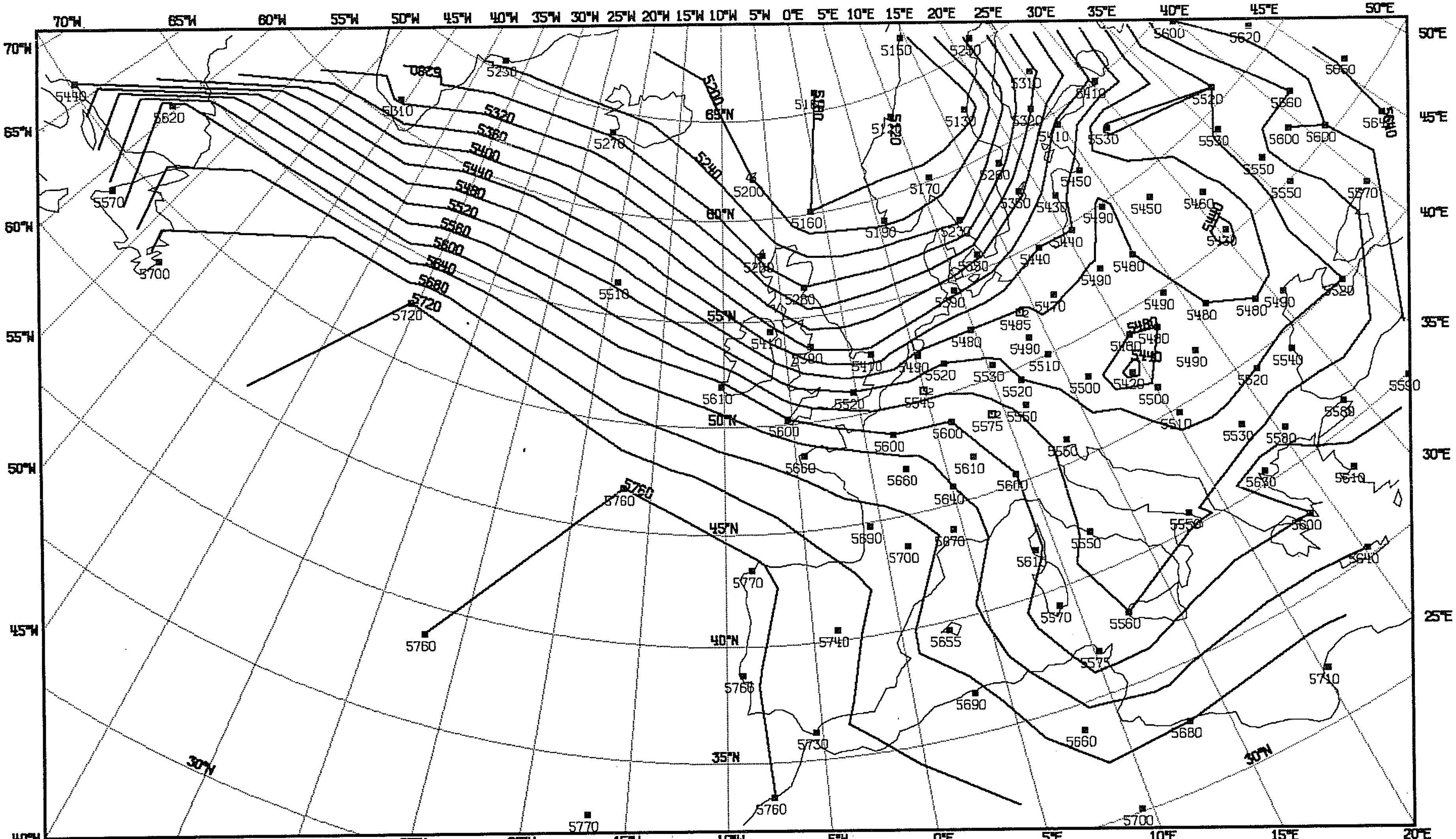

Fig. 17 Direct contouring of 500 mb radiosonde heights at 12Z 1 May 1982.

and vorticity fields.

On the 29th, an area of high vorticity (> .0001 s^{-1}) was centred just west of Denmark. During the next day, the trough extended into central Europe; the vorticity was then drawn into an elongated band extending southward to the Mediterranean. In the further development on the 1st of May, the sharp trough splits the flow into northern and southern Europe branches, see Fig. 16. The vorticity band weakened and broke up into two positive cells, one east of the Alps, the other in the trough around Sicily. The cyclogenic process in the Mediterranean seems more realistic in the forecasts from the 19-level assimilation than for the control (see Figs. 14 & 15). The direct contouring of the 500 mb radiosonde height's, Fig. 17, reveals a sharper anticyclonic curvature over southern France than was present in the operational analysis; in this sense the two forecasts are realistic, though the troughs over Italy are too deep by some 120 m. Another feature is the circulation in the north Atlantic; a secondary low is isolated around Svalbarb Island for the 19 level case (K82) but not for the control (L18).

Further experiments are planned for studying the impact on the boundary layer structure. However an improvement has already been found for the April case in the cold Arctic continents, where unrealistic inversions between the two lowest σ-layers could occur in the first guess temperature fields due to the radiative surface cooling over snow during the 6-hour forecasts. The described experiments suffered from problems in dealing with the extra-level SATEM thicknesses, as described in part 3. The necessary modifications were not included in the experiments reported here.

7. CONCLUSIONS

It has been shown how a higher vertical resolution can be achieved within the framework of the present ECMWF data-assimilation system. A number of highly resolved wind soundings were available for FGGE in a delayed mode; if such

data were part of a future observational network, it would help the user to find the optimum balance between resolution and reliability of the analysis required.

ACKNOWLEDGEMENTS

I thank A.Hollingsworth and D.Shaw for their encouragements and interest in this project, I also benefited from discussions with all members of the ECMWF data-assimilation section.

REFERENCES

Bengtsson, L., 1980 Current Problems in Four-Dimensional Data-Assimilation. ECMWF Seminar 1980, Data Assimilation Methods, 195-217.

Bjornheim, K., Julian, P., Kanamitsu, M., Kallberg, P., Price, P. Tracton, S. Uppala, S., 1981, FGGE III-B Daily Global Analyses. Available from ECMWF.

Hollett, S.R., 1975, Three-dimensional spatial correlations of P.E. forecasts errors. M.Sc. Thesis, McGill University, Montreal, Quebec, Canada, 73pp.

Lönnberg, A., 1982, Structure functions and their implication for high resolution analysis, Workshop on Current Problems in Data Assimilation, ECMWF,

Lorenc, A., Rutherford, I., Larsen, G., 1977 The ECMWF Analysis and Data-Assimilation Scheme. ECMWF Technical Report No. 6.

Lorenc, A., 1981 A global Three-Dimensional Multivariate Statistical Interpolation Scheme.
Monthly Weather Review,Vol.109, No.4,1981.

Tiedtke, M., Geleyn, J-F. Hollingsworth, A., Louis, J-F., 1979, ECMWF model parameterization of sub-grid scale processes. ECMWF Technical Report No 10, 46pp.